

# The Density, Magnetic Properties, Young's Modulus, and E-Effect, and Their Changes Due to Quenching in Ferromagnetic Iron-Aluminium Alloys. I : The Density and Magnetic Properties

著者	YAMAMOTO Mikio, TANIGUCHI Satoshi
journal or publication title	Science reports of the Research Institutes, Tohoku University. Ser. A, Physics, chemistry and metallurgy
volume	8
page range	112-124
year	1956
URL	<a href="http://hdl.handle.net/10097/26758">http://hdl.handle.net/10097/26758</a>

# The Density, Magnetic Properties, Young's Modulus, and $\Delta E$ -Effect, and Their Changes Due to Quenching in Ferromagnetic Iron-Aluminium Alloys. I

## The Density and Magnetic Properties\*

Mikio YAMAMOTO and Satoshi TANIGUCHI

*The Research Institute for Iron, Steel and Other Metals*

(Received February 18, 1956)

### Synopsis

The density and ferromagnetic properties in annealed as well as in quenched states of iron-aluminium alloys containing less than 17%Al have been measured. Densities of alloys containing more than 10%Al decrease by quenching from 700°C, the observed relative changes being in good agreement with values calculated from the data for changes in lattice parameter obtained by Bradley and Jay. The saturation magnetization in alloys containing 10 to 12%Al increases, while that in alloys containing more than 13% Al decrease by quenching, indicating that the  $\text{Fe}_3\text{Al} \rightarrow \text{FeAl}$  transition may accompany a fall in Curie temperature. The magnetization in alloys containing some 17%Al is low, and never attain to saturation even at high fields. It is also shown that the magnetocrystalline anisotropy constant of iron decreases by the addition of aluminium and changes its sign near the  $\text{Fe}_3\text{Al}$  composition.

### I. Introduction

Iron-rich iron-aluminium alloys are well known in virtue of the existence of superlattices  $\text{Fe}_3\text{Al}$  (13.9%Al) and  $\text{FeAl}$  (32.6%Al)<sup>(1)</sup> and of large magnetostriction<sup>(2)</sup>. The iron-side phase diagram of this alloy system accepted at present is shown in Fig. 1<sup>(3)</sup>, which indicates that in slowly cooled state the superlattice  $\text{Fe}_3\text{Al}$  ( $\alpha_1$  phase) whose transition temperature is about 570°C occupies a composition range approximately from 11 to 20 percent aluminium and the superlattice  $\text{FeAl}$  ( $\alpha_2$  phase) exists in a composition range from 20 to 32.6 percent aluminium, while in quenched state the composition ranges less than and more than 13.9 percent aluminium are occupied by a disordered body-centered cubic ( $\alpha$ ) phase and by the ordered  $\alpha_2$  solid solution, respectively. Further, the ferromagnetic Curie point falls with increasing aluminium content and eventually reaches to ordinary temperatures at about 17 percent aluminium.

Physical properties of ferromagnetic iron-aluminium alloys have been the object of a large number of investigations<sup>(3)</sup>, but the  $\Delta E$ -effect has not yet been measured.

\* The 829th report of the Research Institute for Iron, Steel and Other Metals. The original of this report as written in Japanese language was published previously in *Nippon Kinzoku Gakkai-shi* (J. Japan Inst. Metals), **17** (1953), 529 and 532.

(1) A. J. Bradley and A. H. Jay, *Proc. Roy. Soc.*, **A138** (1932), 210; *J. Iron Steel Inst.*, **125** (1932), 339.

(2) V. S. Messkin, B. E. Somin and A. S. Nekhamkin, *J. Tech. Phys. (USSR)*, **11** (1941), 918; K. Honda, H. Masumoto, Y. Shirakawa and T. Kobayashi, *Nippon Kinzoku Gakkai-shi*, **12** (1948), No. 7-12; *Sci. Rep. RITU*, **A1** (1949), 341.

(3) R. M. Bozorth, *Ferromagnetism*, D. Van Nostrand, New York (1951), p. 210.

So, we have studied Young's modulus and the  $\Delta E$ -effect and their changes due to quenching in these alloys, of which the report will be described in Part II of the present paper. In connection with this study, we also have measured the density and ferromagnetic properties and their change due to quenching and found some new interesting facts regarding the influence of the order-disorder transformation in alloys of the  $\text{Fe}_3\text{Al}$  and nearby compositions, which will be reported in the present part.

## II. Specimens and methods of measurements

The specimens used are circular rods of 17 alloys containing less than 17 percent aluminium, of which the chemically analysed compositions are shown in Table 1. The specimens were prepared as follows:— Electrolytic iron and Alcoc aluminium were melted and mixed in a

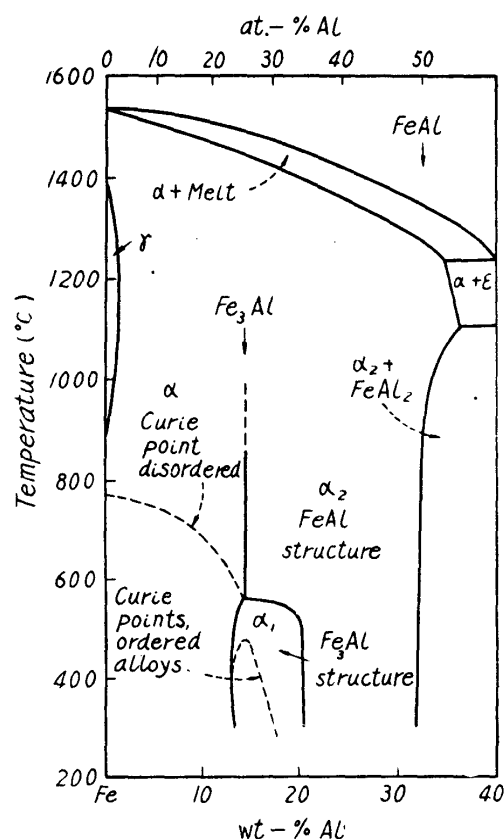


Fig. 1. Phase diagram of iron-rich iron-aluminium alloys.

Table 1. Composition, dimensions, and the measured densities for specimens of iron-aluminium alloys in annealed and in quenched states.

No.	Specimen Mark	Composition wt.-%Al	Annealed state				Quenched state			
			Dimensions (cm)		Density g/cm <sup>3</sup>	Temperature °C	Dimensions (cm)		Density g/cm <sup>3</sup>	Temperature °C
			Length	Diameter			Length	Diameter		
1	1b	0.02	9.970	0.3974	7.835	26.4	—	—	—	—
2	3b	1.22	10.010	0.3982	7.699	26.0	—	—	—	—
3	4	1.83	10.000	0.3987	7.649	27.0	—	—	—	—
4	5a	2.75	10.000	0.3996	7.542	27.0	—	—	—	—
5	6a	4.05	10.000	0.3998	7.265	26.1	—	—	—	—
6	7a	5.46	10.000	0.4009	7.239	20.5	—	—	—	—
7	7b	5.46	10.000	0.3997	7.218	20.3	—	—	—	—
8	9	7.43	10.000	0.3986	7.042	15.0	—	—	—	—
9	10	7.94	10.000	0.4002	7.005	15.8	—	—	—	—
10	N11a	9.53	9.995	0.3009	6.849	14.0	—	—	—	—
11	N11b	9.53	9.995	0.3009	6.855	13.9	—	—	—	—
12	12	11.16	9.970	0.2999	6.778	15.6	9.985	0.3002	6.763	14.3
13	13	12.07	8.965	0.2525	6.723	15.1	8.985	0.2536	6.688	14.1
14	14b	13.15	9.990	0.3000	6.661	15.0	9.995	0.3001	6.649	14.1
15	15	13.92	10.025	0.3987	6.610	16.3	10.020	0.3985	6.609	14.2
16	16a	14.15	10.000	0.2998	6.596	15.3	10.005	0.2999	6.594	14.0
17	16b	14.15	10.000	0.2995	6.599	15.2	—	—	—	—
18	17	14.70	9.995	0.3003	6.545	15.5	10.000	0.3016	6.534	14.0
19	18	16.00	9.995	0.2993	6.478	15.6	9.995	0.2992	6.471	14.0
20	19	16.96	9.990	0.3004	6.430	15.4	9.990	0.3004	6.425	13.8

high-frequency induction furnace, casted into an iron mold, hot-forged well, and lathe-machined into circular rods 3~4 mm in diameter and 10 cm long<sup>(4)</sup>. The results of chemical analysis<sup>(5)</sup> of the raw materials are given in Table 2.

Table 2. Chemical analysis (in weight percent) of the metals used for alloying.

Metal	Fe	C	Si	Mn	P	S	Cu	Al	Zn
Fe (Electrolytic)	—	0.04	0.002	0.015	0.000	0.003	None	0.02	—
Al (Alcoc)	0.48	0.02	0.01	0.008	Trace	0.002	None	—	0.02

The heat-treatments adopted are annealing and quenching. Annealing was made by heating at 1000°C for 2 hours *in vacuo* and subsequent furnace-cooling. This annealing may be considered as perfect, since the order-disorder transition of the superlattice Fe<sub>3</sub>Al is fairly rapid according to previous investigations<sup>(6)</sup>. On the other hand, quenching was made only for alloys containing 11 to 17 percent aluminium as follows: the alloys were heated at 900°C for an hour *in vacuo*, furnace-cooled to 700°C, kept at this temperature for 10 minutes, and then dropped into water.

The density was measured with the weighing-in-water method. The magnetic measurements were made in the range of magnetic field up to about 1100 oersteds with the ballistic-galvanometer method, using a water-jacketed solenoid, of the length of 40 cm, with the coil constant of 58.2 Oe/A. The demagnetizing factors for the annealed and quenched states of a specimen were regarded as the same, though the dimensions were different slightly, as seen from Table 1, corresponding to the change in the density due to quenching. The demagnetizing factors of the specimens adopted are given in Table 3.

### III. The densities

A number of direct measurements have hitherto been made on the densities of iron-rich iron-aluminium alloys<sup>(7~11)</sup>, and some determinations of their lattice constants<sup>(1,8,12)</sup> are also available. As shown in Fig. 2, the directly measured values

- (4) The raw materials and some of the specimens used were furnished from Prof. H. Masumoto, to whom the authors are much indebted.
- (5) The chemical analysis was made at the chemical analysis laboratory of our Research Institute.
- (6) Cf. for instance, T. Kubo, *Nippon Sôgaku Buturigaku Kaishi*, **16** (1942), 426 (in Japanese).
- (7) E. Gumlich, *Stahl u. Eisen*, **39** (1919), 901 (0.5~10.5%Al, the rolled state).
- (8) Z. Nishiyama, *Sci. Rep. Tôhoku Univ.*, **18** (1929), 359 (0~14%Al; annealed at 900°C for 2 hours).
- (9) F. Wever and A. Müller, *Z. anorg. allg. Chem.*, **192** (1930), 337 (4.4, 7.1 and 11.5%Al; annealed at 950°C).
- (10) C. Sykes and J. W. Bampfylde, *J. Iron Steel Inst.*, **130** (1934), 389 (0~16%Al; the state unknown).
- (11) H. Masumoto and H. Saito, *Nippon Kinzoku Gakkai-shi*, **8** (1944), 359; *Sci. Rep. RITU*, **A3** (1951), 523 (0~17%Al; heated at 1000°C for an hour, furnace cooled to 700°C, and then cooled with the rate of 30°C/hr).
- (12) A. Ôsawa and T. Murata, *Nippon Kinzoku Gakkai-shi*, **5** (1941), 529 (in Japanese).

of the densities,  $\rho$ , are in good agreement with the values of densities calculated from the relation between the density and lattice constant,  $a$ , for the body-centered cubic solid solution

$$\rho = 2M/Na^3, \quad (1)$$

where  $M$  is the mean atomic weight of an alloy and  $N$  the Avogadro number, except for Nishiyama's<sup>(8)</sup> X-ray measurements. Thus, it has been established that the density of iron (7.86~7.87 g/cm<sup>3</sup>) first decreases

linearly with an addition of aluminium and attains a value of approximately 7.1 g/cm<sup>3</sup> at 7 percent aluminium, the rate of decrease diminishes slightly near 10 percent aluminium and then the density decreases again linearly and attains to approximately 6.5 g/cm<sup>3</sup> at 16 percent aluminium (Fig. 2).

Now, as mentioned above, iron-aluminium alloys containing 11 to 20 percent aluminium undergo the order-disorder transition, and how does this transition affect on the density? According to X-ray investigations by Bradley and Jay<sup>(1)</sup> and by Ôsawa and Murata<sup>(12)</sup>, the lattice constants of these alloys increase by quenching from temperatures above the transition temperatures, 14%Al alloy showing a maximum value of relative increase of 0.1~0.2 percent. Then, since it follows from Eq. (1) that

$$\Delta\rho/\rho = -3\Delta a/a, \quad (2)$$

the densities of these alloys should decrease by quenching and the relative decrease in density of 14%Al alloy should amount to 0.3~0.5 percent, which is the magnitude to be detected by a direct measurement of the density.

The results of our direct measurements on the densities in annealed and in quenched states of iron-aluminium alloys containing less than 17 percent aluminium are given in Table 1. The composition dependence of the density in annealed state (Fig. 3) is in a good agreement

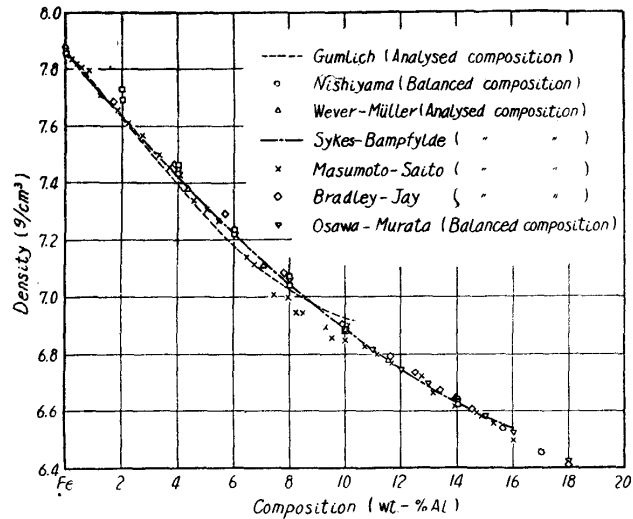


Fig. 2. Various data on the densities of iron-rich iron-aluminium alloys.

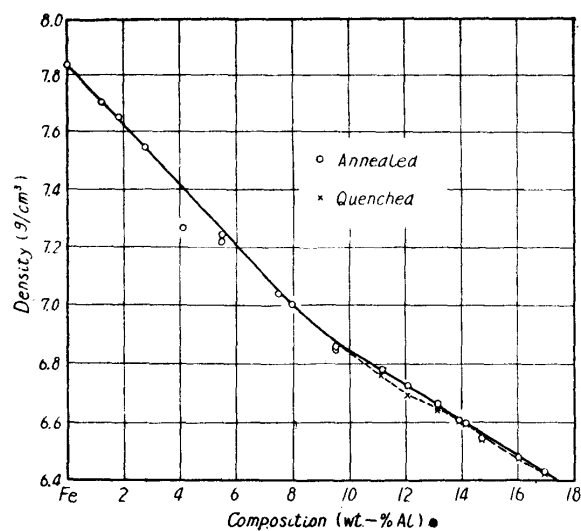


Fig. 3. Density as a function of the composition in iron-rich iron-aluminium alloys (the present authors).

with the hitherto obtained results of direct and indirect determinations shown in Fig. 2. The densities of alloys containing more than 10 percent aluminium are decreased by quenching from 700°C (Table 1 and Fig. 3). The relative decrease of the density is as shown by a solid line in Fig. 4; it shows a maximum of 0.5 percent at about 12 percent aluminium and becomes very small once at about 14 percent aluminium, but it becomes larger again with further increasing aluminium content and then decrease gradually. These results of our direct measurements agree well with the results of Bradley and Jay's<sup>(1)</sup> X-ray investigation, excepting for slight relative deviations of the composition, as seen from Fig. 4.

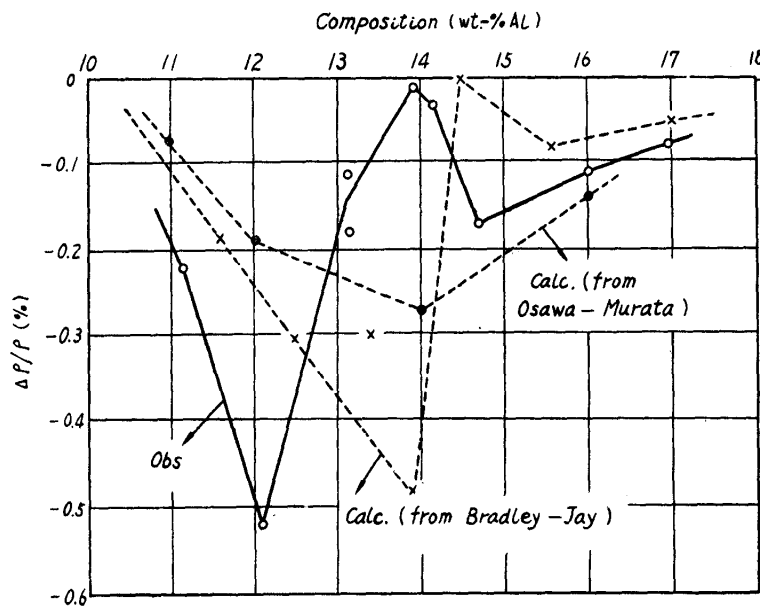


Fig. 4. Change in density due to quenching from 700°C, relative to that in annealed state, in iron-aluminium alloys containing 10 to 18 percent aluminium.

From the comparison of results of our density measurements and of Bradley and Jay's<sup>(1)</sup> X-ray investigation, it may be considered that our alloy specimens in annealed state containing more than about 10 percent aluminium belong to the  $\text{Fe}_3\text{Al}$  phase and the rest specimens to the disordered  $\alpha$  phase, while in quenched state the specimens containing more than about 13 percent aluminium occupy the  $\text{FeAl}$  phase, the rest specimens having the disordered  $\alpha$  phase.

#### IV. The magnetic properties

##### A. Magnetization curves

The representative magnetization curves for annealed and for quenched states are shown in Figs. 5 and 6. Fig. 7 shows the composition-dependence of the intensities of magnetization for (effective) magnetic fields of 1, 3, 5, 10, 20, 50, 100, 300 and 800 Oe. As seen from Fig. 7(a), the magnetization at low fields in annealed state exhibits minima at the boundary between the disordered  $\alpha$  phase and ordered  $\alpha_1$  phase (about 10 percent aluminium) and at about 14 percent aluminium and maxima at about 12 and 14 percent aluminium. As the field increases, these minima

and maxima become more and more flat and eventually the magnetization at high fields over 800 Oe vs. composition curves fall monotonously with increasing aluminium content, except for a small kink at about 14 percent aluminium. By being quenched, the magnetization at low fields vs. composition curves for the composition range from approximately 10 to 14 percent aluminium change completely their appearance (Fig. 7(b)) and they show maxima centered at about 14 percent aluminium. These maxima also become flat as the field increases, and the magnetization at high fields over 800 Oe vs. composition curves fall almost monotonously with increasing aluminium content.

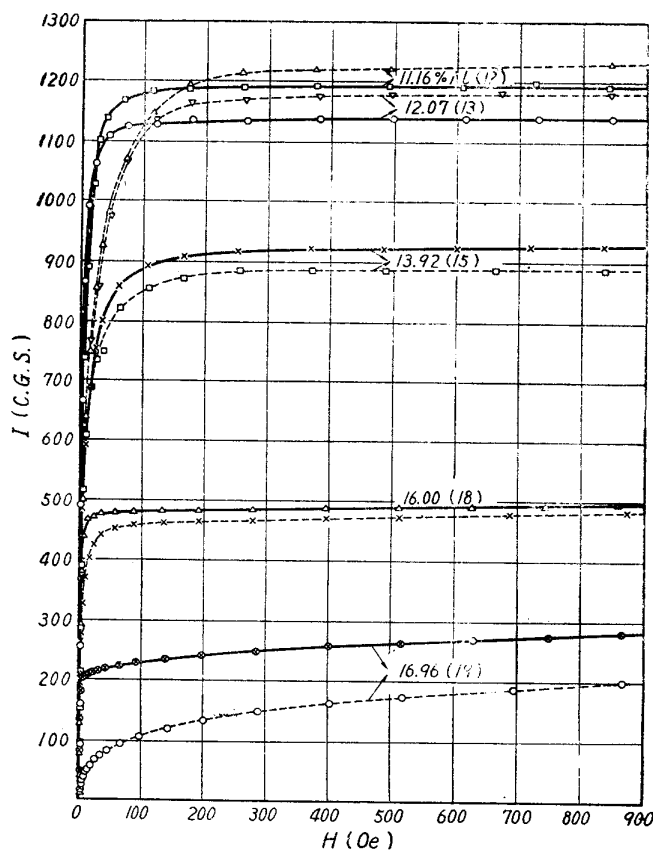


Fig. 6(a). Magnetization curves of iron-aluminium alloys containing from 11 to 17 percent aluminium in annealed and in quenched states. — annealed, --- quenched.

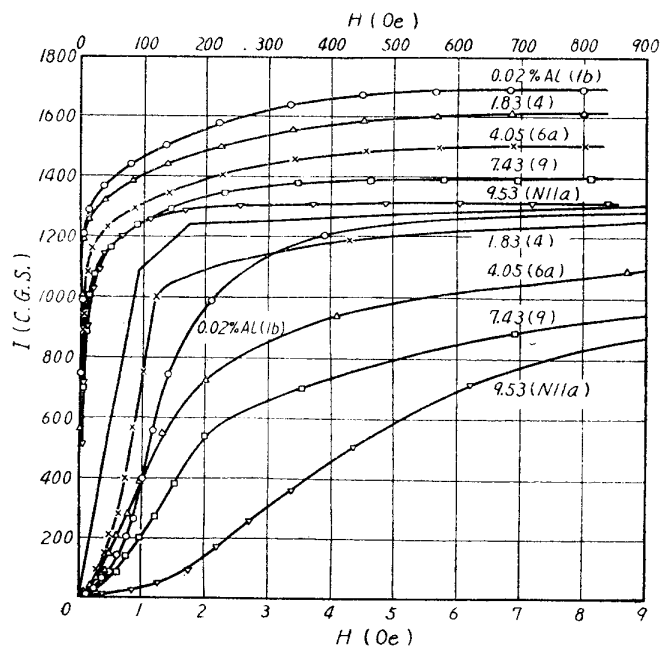


Fig. 5. Magnetization curves of annealed iron-aluminium alloys containing less than 10 percent aluminium.

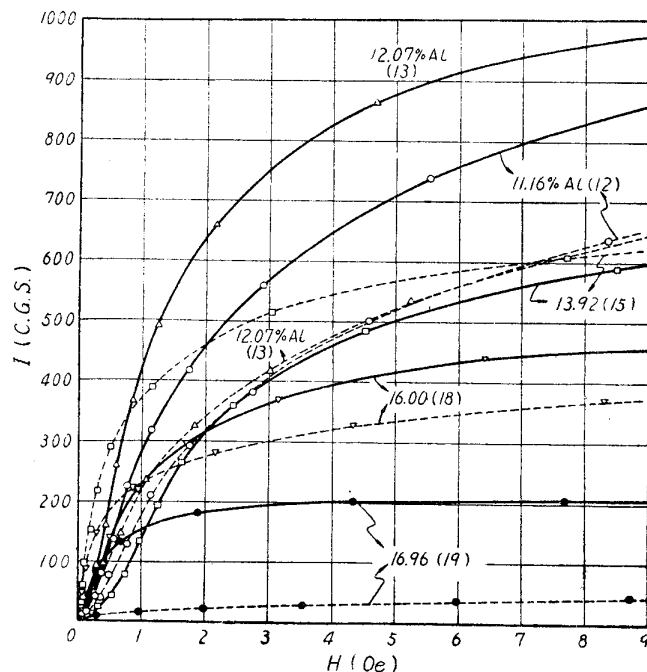


Fig. 6(b). Magnetization curves at low fields of iron-aluminium alloys containing 11 to 17 percent aluminium in annealed and in quenched states. — annealed, --- quenched.

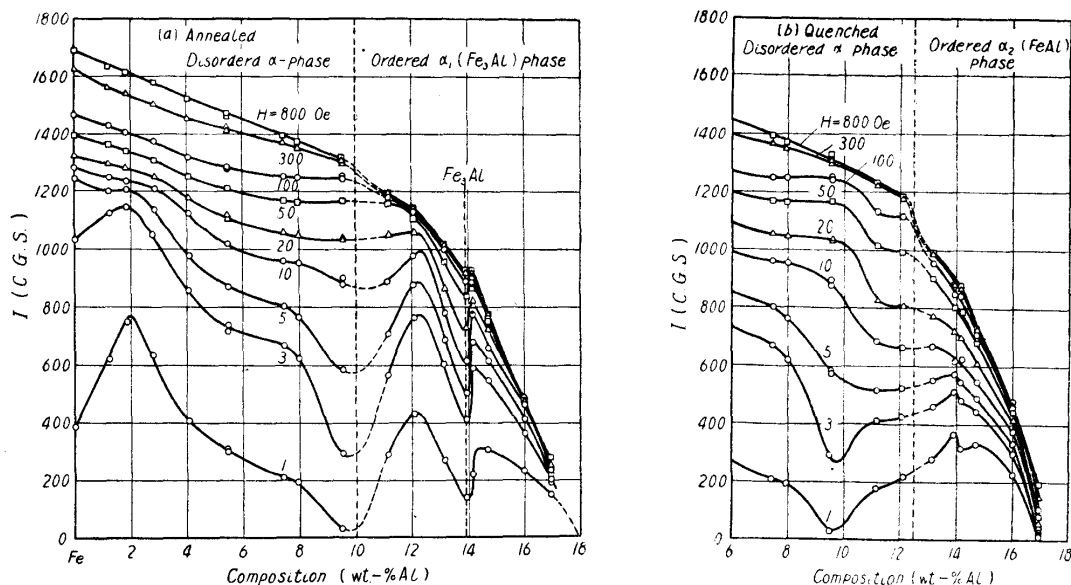


Fig. 7. Magnetization,  $I$ , for various constant fields as dependent on the composition in iron-aluminium alloys.  
(a) Annealed state, (b) quenched state.

Fig. 7 indicates, further, that the composition where the magnetization vanishes at ordinary temperatures is about 18 percent aluminium for annealed alloys, namely for the ordered  $\alpha_1$  phase, and about 17.5 percent aluminium for quenched alloys, namely for the ordered  $\alpha_2$  phase. It is to be noted, further more, that quenching causes an increase of the saturation magnetization in alloys containing less than about 12.5 percent aluminium and a decrease in the remaining alloys, as seen from Fig. 6(a) and Table 3.

Finally, as seen also from Fig. 6(a), the magnetization curves of annealed alloys containing more than about 13 percent aluminium and of quenched alloys containing more than about 11 percent aluminium do not attain to saturation at high fields but rises approximately linearly with field. This effect is most conspicuous for 17 percent aluminium alloy and, in particular, the high-field portion of its magnetization curve for quenched state shows a bending similar to that of nickel near the Curie temperature<sup>(13)</sup>, corresponding to the above-mentioned lowering of the composition bordering the ferromagnetic phase or a lowering of the Curie temperature.

#### B. Initial and maximum magnetic susceptibilities

The maximum magnetic susceptibility,  $\chi_{max}$ , was determined from the magnetization curve, while the initial susceptibility,  $\chi_0$ , was determined by separate measurements in very low fields. The measured values for  $\chi_0$  and  $\chi_{max}$  in annealed and in quenched states are given in Table 3. The composition dependences of  $\chi_0$  and of  $\chi_{max}$  are similar to each other, as shown in Fig. 8, and correspond well with that of the magnetization at low fields (Fig. 7). It is to be noted that in quenched state conspicuous maxima with a saddle centered at about 14 percent aluminium

(13) P. Weiss and R. Forrer, *Ann. de physique*, 5 (1926), 153.



Table 3. Composition, demagnetizing factor, and the measured and computed magnetic quantities for specimens of iron-aluminium alloys in annealed and in quenched states.

No.	Specimen Mark	Composition wt.-% Al	Demagnetizing factor	Annealed state				Quenched state					
				$\chi_0$	$\chi_{max}$	$I_s$ C. G. S.	$H_s$ Oe	$K$ $10^5\text{erg/cm}^3$	$\chi_0$	$\chi_{m.s.}$	$I_s$ C. G. S.	$H_s$ Oe	$K$ $10^5\text{erg/cm}^3$
1	1b	0.02	0.0451	24.0	533	1696	1000	4.2	—	—	—	—	—
2	3b	1.22	0.0450	47.8	631	1635	1000	4.1	—	—	—	—	—
3	4	1.83	0.0450	56.7	748	1618	960	3.9	—	—	—	—	—
4	5a	2.75	0.0454	58.8	635	1580	930	3.9	—	—	—	—	—
5	6a	4.05	0.0455	24.6	420	1520	930	3.5	—	—	—	—	—
6	7a	5.46	0.0457	30.0	337	1471	900	3.3	—	—	—	—	—
7	7b	5.46	0.0454	41.9	324	1465	900	3.3	—	—	—	—	—
8	9	7.43	0.0450	31.2	271	1397	900	3.1	—	—	—	—	—
9	10	7.94	0.0457	37.8	298	1372	850	2.9	—	—	—	—	—
10	N11a	9.53	0.0282	13.64	117.3	1323	900	3.0	—	—	—	—	—
11	N11b	9.53	0.0282	14.28	115.4	1310	750	2.5	—	—	—	—	—
12	12	11.16	0.0281	91.0	289	1194	650	1.9	31.6	227	1222	500	1.5
13	13	12.07	0.0249	115.7	600	1140	500	1.7	41.6	219	1176	450	1.3
14	14b	13.15	0.0280	71.2	287	1021	400	1.0	109.5	483	992	450	1.1
15	15	13.92	0.0450	49.2	164	911	250	-0.57	111	1267	883	350	0.77
16	16a	14.15	0.0279	58.4	266	915	350	-0.80	94	694	865	300	-0.65
17	16b	14.15	0.0279	51.9	266	906	270	-0.61	—	—	—	—	—
18	17	14.70	0.0280	51.7	308	767	400	-0.77	139	947	731	450	-0.82
19	18	16.00	0.0279	53.7	279	480	350	-0.42	167	962	461	300	-0.35
20	19	16.96	0.0281	80.6	307	237	300	-0.18	52.1	108.9	—	—	—

appear in a composition range from 12 to 17 percent aluminium.

Our results of measurements on  $\chi_0$  and  $\chi_{max}$  are in a qualitatively and roughly good agreement with those obtained by Masumoto and Saito<sup>(14)</sup>. A part of large quantitative discrepancies for annealed state may be considered as due to the difference in the condition of heat-treatment employed by us and by them<sup>(11)</sup>. It is to be noted, further, that the maxima at about 2 percent aluminium of  $\chi_0$  and  $\chi_{max}$  observed by us (Fig. 8) may probably be due to the effect of deoxidation by aluminium during melting of alloys.

### C. Saturation magnetization, saturation magnetic field, and magnetocrystalline anisotropy energy

The saturation magnetization,  $I_s$ , and saturation magnetic field,  $H_s$ , were determined from the measured magnetization curves. For aluminium-rich alloys, of which the magnetization curves rise approximately linearly at high fields, as mentioned in A, the linear portion of a magnetization curve was extrapolated to zero field to determine the value of  $I_s$  and the field where the linear portion deviates from the magnetization curve was taken as  $H_s$ . Thus determined values of  $I_s$  and  $H_s$  are given in Table 3.

In order to compare these data with hitherto obtained ones, the specific saturation magnetic moment  $\sigma_s$  ( $= I_s/\rho$ ,  $\rho$ : density), was also calculated. Fig. 9 shows  $\sigma_s$  as a

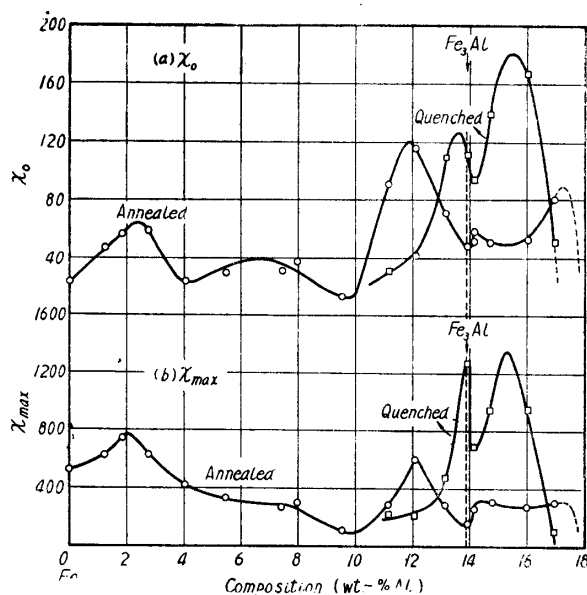


Fig. 8. Initial and maximum magnetic susceptibilities,  $\chi_0$  and  $\chi_{max}$ , as dependent on the composition in iron-aluminium alloys in annealed and in quenched states.

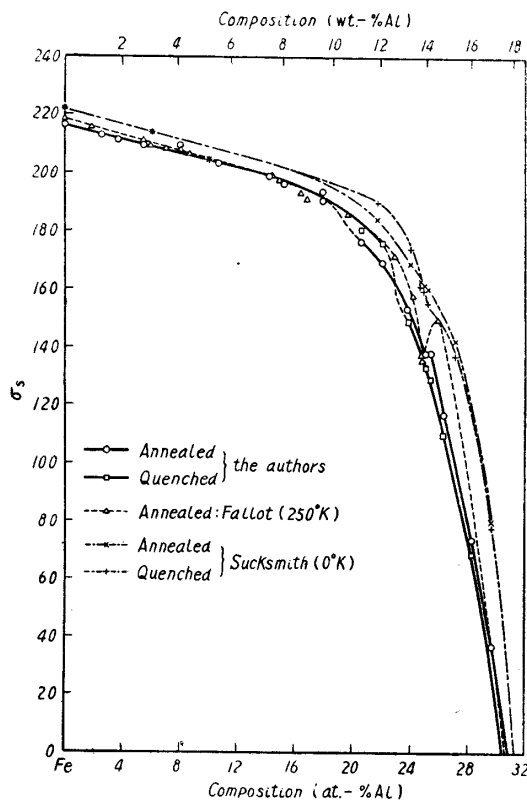


Fig. 9. Saturation magnetic moment per unit mass,  $\sigma_s$ , as dependent on the composition in iron-aluminium alloys in annealed and in quenched states.

(14) H. Masumoto and H. Saito, *Nippon Kinzoku Gakkai-shi*, **6**(1942), 123; **8**(1944), 359; **12**(1948), No. 5; **B14**(1950), No. 5; *Sci. Rep. RITU*, **A3**(1951), 523; **A4**(1952), 321, 338.

function of the composition expressed in atomic percent, which indicates that with increasing aluminium content  $I_s$  or  $\sigma_s$ , in annealed state decreases almost linearly in the begining and more and more quickly over about 18 atomic-percent (10 weight-percent) aluminium, vanishing at about 31 atomic-percent (18 weight-percent) aluminium. This general trend is similar to the results so far obtained<sup>(15-18)</sup>.

It is to be noted, however, that our results indicate an irregularity near the  $\text{Fe}_3\text{Al}$  composition (13.9%Al), which is seen quite distinctly in Fallot's<sup>(15)</sup> data. On the other hand, the first linear decrease of  $I_s$  or  $\sigma_s$  with increasing aluminium content is extended up to about 12 percent aluminium (about 22 atomic percent) by quenching and  $I_s$  or  $\sigma_s$  for quenched state shows a rapid decrease at 12~13 percent aluminium, so that the  $I_s$  or  $\sigma_s$  vs. composition curve for annealed and quenched states crosses at about 13 percent aluminium. Further, quenching obliterates the above-mentioned irregularity near the  $\text{Fe}_3\text{Al}$  composition of the curve for annealed state.

As seen also from Fig. 9, in the low aluminium range, Fallot's<sup>(15)</sup> data for  $\sigma_s$  at 250°K are slightly higher than, but go parallel with, ours, and it may be said that both data are in good agreement with each other. But, as the aluminium content exceeds over about 18 atomic percent, they differ considerably, and, moreover, the irregular change of  $\sigma_s$  near the  $\text{Fe}_3\text{Al}$  composition observed by Fallot is much more conspicuous than that by us. These differences may be interpreted as caused primarily by the difference of the procedures of determining  $\sigma_s$  adopted by Fallot and by us. Fallot<sup>(15)</sup> assumed that the field dependency of the specific magnetic moment,  $\sigma_H$ , at high fields may be expressed as

$$\sigma_H = \sigma_s (1 - a/H), \quad (3)$$

where  $H$  is the magnetic field and  $a$  is a constant, and he determined the value of  $\sigma_s$ , by extrapolating this relation to  $H = \infty$ . It is to be noticed, however, that the rise at high fields of the magnetization curves of high-aluminium alloys may not be due to  $a/H$  in Eq. (3) but to the increase in the spontaneous magnetization caused by the direct influence of magnetic field. Because, according to our measurements, the rise of magnetization at high fields is most conspicuous for 17%Al alloy of which the Curie point is the lowest (cf. Fig. 6(a)). Thus, it may be more correct to determine the value of  $\sigma_s$  by extrapolating the linear portion at high fields of the magnetization curve as we have done.

Comparison between the change in saturation magnetization at 0°K due to quenching from 900°C as determined by Sucksmith<sup>(17)</sup> using the same procedure as ours with the change in saturation magnetization at ordinary temperatures due to quenching from 700°C as determined by us is shown in Fig. 10, which indicates that both results are in good agreement with each other except for slight relative

(15) M. Fallot, *Ann. de physique*, **6** (1936), 305.

(16) W. S. Messkin and B. E. Somin, *Z. Phys.*, **98** (1936), 610.

(17) W. Sucksmith, *Proc. Roy. Soc.*, **A171** (1939), 525.

(18) K. Honda, H. Masumoto, Y. Shirakawa and T. Kobayashi, *Nippon Kinzoku Gakkaishi*, **12** (1948), No. 7~12; *Sci. Rep. RITU*, **A1** (1949), 341.

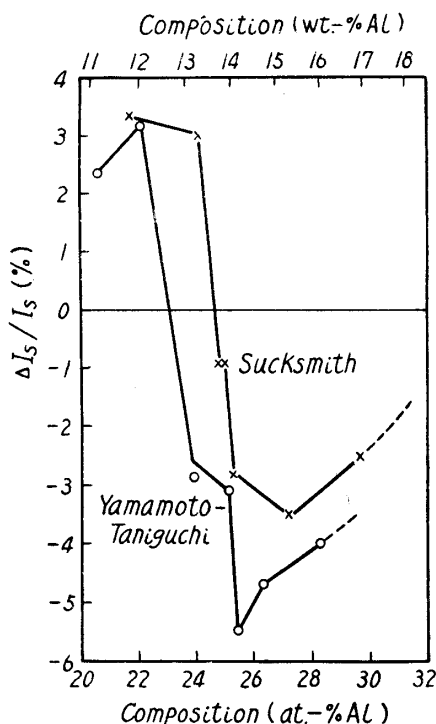


Fig. 10. Change in saturation magnetization due to quenching from 700°C, relative to that at annealed state, in iron-aluminium alloys containing 21 to 30 atomic percent aluminium.

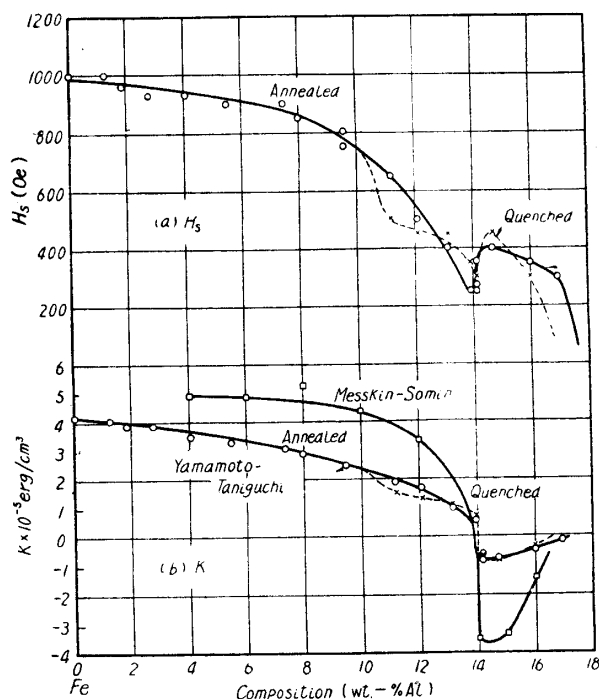


Fig. 11. Saturation field,  $H_s$ , and magnetocrystalline anisotropy constant,  $K$ , as dependent on the composition in iron-aluminium alloys in annealed and in quenched states.

deviations in the composition. It is to be noticed that alloys containing approximately 10~12 percent aluminium showing an increase in saturation magnetization due to quenching undergo the order-disorder transformation of superlattice  $\text{Fe}_3\text{Al}$  and alloys containing more than about 13 percent aluminium showing a decrease in saturation magnetization due to quenching undergo the  $\text{FeAl} \leftrightarrow \text{Fe}_3\text{Al}$  transformation.

The saturation field,  $H_s$ , decreases more and more rapidly with increasing aluminium content and once exhibits a minimum near 14 percent aluminium (Fig. 11(a)). By quenching  $H_s$  decreases for alloys containing less than about 12 percent aluminium and more than about 14 percent aluminium and increase for alloys of intermediate compositions, but the minimum of  $H_s$  near 14 percent aluminium is not obliterated. Since a minimum of the saturation field in the solid solution range generally means a change in the sign of the (first) ferromagnetic anisotropy constant,  $K$ , it may be inferred that  $K$  changes from positive to negative near the  $\text{Fe}_3\text{Al}$  composition.

Finally, the (first) ferromagnetic anisotropy constant,  $K$ , was computed by a formula:

$$|K| = I_s H_s / 4, \quad (4)$$

which had been found to agree well with the measured data for nickel-cobalt<sup>(19)</sup> and nickel-copper<sup>(20)</sup> alloys and had also been based on a theo-

(19) M. Yamamoto, Nippon Kinzoku Gakkai-shi, **11** (1947), No. 11-12; **13** (1949), No. 6; Sci. Rep. RITU, **A4** (1952), 14.

(20) M. Yamamoto, Sci. Rep. RITU, **A6** (1954), 446.

retical ground<sup>(21)</sup>. The computed data are given in Table 3 and plotted in Fig. 11(b). It may be seen that the computed value for iron is in good agreement with the measured values<sup>(22)</sup>. Taking into considerations of the above-mentioned inference from the trend of the  $H_s$  vs. composition curve, it may be concluded that  $K$  decreases with increasing aluminium content and changes from positive to negative near the  $\text{Fe}_3\text{Al}$  composition, but soon tends to become zero. This course is in a qualitative agreement with the results obtained by Messkin and Somin<sup>(16)</sup> using an approximate formula  $|K| = 5 \int_0^{I_s} H dI$  for polycrystalline specimens (Fig. 11(b)), though they consider  $K$  as positive for alloys near the  $\text{Fe}_3\text{Al}$  composition. Further, Went<sup>(23)</sup> determined  $K$  values from the shape of ideal magnetization curve for polycrystalline specimens, and suggested that  $K$  passes through zero at about 12 percent aluminium. It is to be noted, finally, that quenching displaces the composition at which  $K$  passes through zero slightly to the aluminium-rich side.

### Summary

The density and ferromagnetic properties in annealed as well as in quenched states of iron-aluminium alloys containing less than 17 percent aluminium have been measured, respectively, with the weighing-in-water method and with the ballistic method.

Densities of alloys containing more than 10 percent aluminium decrease by quenching from 700°C and the relative change amounts to -0.5 percent for 12 percent aluminium alloy. The observed relative changes have been found to be in good agreement with values calculated from the data for changes in lattice parameter obtained by Bradley and Jay<sup>(1)</sup>.

The initial and maximum susceptibilities,  $\chi_0$  and  $\chi_{max}$ , as functions of the aluminium content show minima at the boundary between the disordered  $\alpha$  phase and ordered  $\text{Fe}_3\text{Al}$  phase (about 10 percent aluminium), common to annealed and to quenched states.  $\chi_0$  and  $\chi_{max}$  for annealed state, in addition, shows minima at about 14 percent aluminium (near the  $\text{Fe}_3\text{Al}$  composition) and maxima at about 12 and 14 percent aluminium, which are replaced by conspicuous maxima with a saddle centered at about 14 percent aluminium in quenched state.

The saturation magnetization,  $I_s$ , in annealed state exhibits an irregularity near the  $\text{Fe}_3\text{Al}$  composition, which is obliterated by quenching. By being quenched, the first linear decrease of  $I_s$  with increasing aluminium content is extended from about 10 to about 12 percent aluminium and the further rapid decrease of  $I_s$  is accelerated, so that the  $I_s$  vs. composition curves for annealed and quenched states crosses at about 13 percent aluminium, corresponding to the fact that alloys containing approximately 10 to 12 percent aluminium show the order-disorder transition

(21) M. Yamamoto, J. Phys. Soc., **10** (1955), 725.

(22) See, for instance, R.M. Bozorth, *Ferromagnetism*, p. 567.

(23) J. J. Went, cited by J. L. Snoek, *New Developments in Ferromagnetic Materials*, Elsevier (1949), p. 16.

of  $\text{Fe}_3\text{Al}$  superlattice and alloys containing more than about 13 percent aluminium the  $\text{FeAl} \longleftrightarrow \text{Fe}_3\text{Al}$  transition.

The saturation field,  $H_s$ , decreases more and more rapidly with increasing aluminium content and once exhibits a minimum near the  $\text{Fe}_3\text{Al}$  composition. Quenching decreases  $H_s$  for alloys containing less than about 12 percent aluminium and more than about 14 percent aluminium and increases  $H_s$  for alloy of intermediate compositions, but does not obliterate the minimum of  $H_s$ , indicating that the cubic anisotropy constant decreases by the addition of aluminium and changes its sign near the  $\text{Fe}_3\text{Al}$  composition.

It is to be noted, finally, that the magnetization in alloy containing some 17 percent aluminium is low and never attains to saturation even at high fields.